Creation of a squeezed photon distribution using artificial atoms with broken inversion symmetry

Martin Koppenhöfer and Michael Marthaler
Institut für Theoretische Festkörperphysik, Karlsruhe Institute of Technology, D-76131 Karlsruhe, Germany
(Received 20 October 2015; revised manuscript received 22 November 2015; published 22 February 2016)

We consider a two-level system with both a transversal and a longitudinal coupling to the electromagnetic field of a resonator. Using a polaron transformation, this Hamiltonian can be mapped onto a Jaynes-Cummings Hamiltonian with generalized field operators acting on the electromagnetic field in the resonator. In contrast to the usual ladder operators a and $a^\dagger$, these operators exhibit a nonmonotonous coupling strength with respect to the number n of photons in the resonator. In particular, there are roots of the coupling between qubit and resonator at certain photon numbers n_0. We show that this effect can be exploited to generate photon-number squeezed light, characterized by a Fano factor $F \ll 1$, with a large number of photons (e.g., of the order of 1×10^4).

DOI: 10.1103/PhysRevA.93.023831

I. INTRODUCTION

Lasers serve as the source of coherent light in spectroscopic and interferometric measurements. The precision of these measurements is fundamentally limited due to shot noise caused by the quantized nature of light and the photon statistics of the radiation source. To circumvent this limitation, squeezed light has been theoretically proposed [1–6] and successfully applied in physical [7–9] and biological experiments [10,11].

To create squeezed light, nonlinear processes are necessary. In the optical regime, squeezed light is created using a conventional laser as the input source for a nonlinear optical material that exploits higher-order processes like wave mixing or parametric down-conversion [12–14] to create squeezed light. In the microwave regime, superconducting parametric devices and nonlinear oscillators have been demonstrated and are being used for parametric [15,16] and bifurcation amplification [17]. It is even possible to build nonlinear superconducting oscillators in the quantum regime [18–20]. However, while parametric processes can be used to generate quadrature squeezing, in this work we study the creation of a squeezed photon distribution [21].

A laser uses atoms as an active medium to create photons. For natural atoms, all diagonal matrix elements of the dipole coupling between cavity and atom vanish because of the inversion symmetry of the atomic Coulomb potential. In terms of a Jaynes-Cummings model, this means that there is a pure σ_x coupling to the radiation field. However, every setup that breaks inversion symmetry will exhibit an additional σ_z coupling to the radiation field. As we show below, this gives rise to photon-number squeezing already in leading order. Such σ_z couplings exist, for instance, in superconducting circuits [22], quantum dots [23], and molecules [24]. It has been shown that a quantum dot with broken inversion symmetry in a microcavity acts as a nonlinear optical element [25]. Lasing with organic molecules is a very applied research field [26] and lasing devices based on solid-state qubits have been studied [27,28]. For superconducting devices, nonlinearities based on the Josephson effect have been proposed as a way to create squeezed photon distributions [29–31]. In experimentally realized lasing devices using superconducting qubits [32–34] or gate-defined double dots [35], the σ_z coupling between an artificial atom and a cavity field is present but has not yet been studied. In addition, the average number of photons in the laser cavity is quite low (e.g., <200 in Ref. [33]).

In this paper, we examine a system described by a general Hamiltonian including both a σ_x and a σ_z coupling between atom and radiation field. Using a polaron transformation, the general Hamiltonian can be mapped onto a Jaynes-Cummings Hamiltonian with generalized field operators that exhibit a nonmonotonous coupling strength with respect to the number n of photons in the resonator (see inset in Fig. 1). If population inversion is established, the photon number in the cavity starts to increase. The stationary average photon number in the laser cavity is given by the balance of photon creation and photon loss rates in the system. Near n_0, the position of the root of the generalized field operator, the photon creation process breaks down because of the decreasing coupling between atom and resonator. This establishes a squeezed photon distribution with an average photon number of the order of n_0. The average photon number can be very large, e.g., of the order of 1×10^4, for realistic parameters. Simultaneously, a strong squeezing, characterized by a Fano factor of $F \ll 1$, can be reached (see Fig. 1).

II. HAMILTONIAN

The system under consideration is described by a Hamiltonian consisting of an artificial atom modeled by a two-level system, interacting with the quantized electromagnetic field of a resonator:

$$H = \tfrac{1}{2}\epsilon\sigma_z + \hbar\omega a^\dagger a + \hbar g[\cos(\theta)\sigma_z + \sin(\theta)\sigma_x](a + a^\dagger). \tag{1}$$

A generalization to an arbitrary number of atoms follows below. The operators σ_i with $i \in \{x,y,z\}$ denote the Pauli matrices, a ($a^\dagger$) is the annihilation (creation) operator of a photon with frequency ω, and ϵ is the level-splitting energy of the two-level system. The photon field and the two-level system are coupled with coupling strength g. In contrast to the standard Jaynes-Cummings model, our system has both a transversal and a longitudinal coupling to the electromagnetic field. The relative coupling strength is characterized by the angle θ.

Equation (1) describes an effective lasing Hamiltonian, where we did not explicitly consider the third state which we

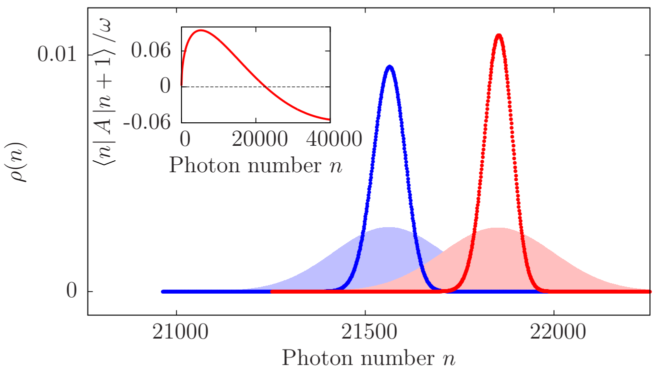

FIG. 1. Photon statistics $\rho(n)$ in the polaron frame for $g = 0.0067, \theta = \pi/10, \Gamma_\uparrow = 0.006, \Gamma_\downarrow = 0.0001, \Gamma_\varphi^* = 0.001$, and $\Delta = 0$. Red dots, one atom, $\kappa = 1 \times 10^{-7}$; blue dots, 100 atoms, $\kappa = 1 \times 10^{-5}$, $S_z^k = 25.8$. All rates and couplings are given in units of ω. The distributions correspond to a Fano factor $F_0 = 0.0621$ and $F_0 = 0.0819$ in the polaron frame, respectively. The Fano factor in the photon-number frame, F, is enhanced by corrections due to the polaron transformation, yielding $F = 0.0622$ and $F = 0.1442$ (strongly squeezed light), respectively. The average photon number is $\langle n\rangle = 21\,851$ and $\langle n\rangle = 21\,562$, respectively. Filled faint red and blue curves represent the photon statistics of an ordinary laser producing classical light with the same average photon number $\langle n\rangle$. Inset: Coupling matrix element $\langle n|A|n+1\rangle$. The root at the photon number $n_0 = 22\,599$ causes the squeezed photon states.

need to establish population inversion. The pumping process is modeled by a Lindblad term in the master equation of this system and is described below. It contains the effective pumping rates between the upper and the lower lasing states.

The Hamiltonian (1) can be mapped onto the well-known Jaynes-Cummings Hamiltonian using the polaron transformation

$$U = \exp[ip\sigma_z] = \exp\left[\frac{g}{\omega}\cos(\theta)(a - a^\dagger)\sigma_z\right].$$

For convenience, we introduce the operators

$$x = x_0(a^\dagger + a) = \hbar g \sin(\theta)(a^\dagger + a),$$
$$p = ip_0(a^\dagger - a) = i\frac{g}{\omega}\cos(\theta)(a^\dagger - a).$$

The transformation yields

$$H_\mathrm{p} = U^\dagger H U = \tfrac{1}{2}\epsilon\sigma_z + \hbar\omega a^\dagger a + (\sigma_+ A + \sigma_- A^\dagger) \qquad (2)$$

with the operators $A = e^{-ip}xe^{-ip}$ and $A^\dagger = e^{ip}xe^{ip}$ instead of the pure annihilation and creation operators known from the Jaynes-Cummings Hamiltonian.

As basis we choose the direct product of the resonator states, $a^\dagger a|n\rangle = n|n\rangle$, and the states of the two-level system, $\sigma_z|\uparrow,\downarrow\rangle = \pm|\uparrow,\downarrow\rangle$. The state $|n\rangle$ is defined in the polaron frame, $|n\rangle|\sigma\rangle = U^\dagger|n\rangle_\mathrm{c}|\sigma\rangle$, where $|n\rangle_\mathrm{c}$ is the state with exactly n photons in the resonator cavity. The matrix elements of A ($A^\dagger$) are purely real and can be expressed in terms of the generalized Laguerre polynomials,

$$\langle n|A^{(\dagger)}|n+m\rangle = \pm\frac{m}{2}\frac{x_0}{p_0}T_{n,m}^\pm, \qquad (3)$$

with $A^\dagger$ taking the upper sign and $n \in \mathbb{N}$, $m \in \mathbb{Z}$, $m \geqslant -n$. For $0 < m < \infty$, $T_{n,m}^\pm$ is given by

$$T_{n,m}^\pm = \langle n|e^{\pm 2ip}|n+m\rangle$$
$$= (\pm 1)^m e^{-2p_0^2}(2p_0)^m\sqrt{\frac{n!}{(n+m)!}}L_n^m(4p_0^2),$$

where $L_n^m(x)$ are the associated Laguerre polynomials. For $-n \leqslant m < 0$, one finds

$$T_{n,m}^\pm = \langle n|e^{\pm 2ip}|n+m\rangle$$
$$= (\mp 1)^{|m|}e^{-2p_0^2}(2p_0)^{|m|}\sqrt{\frac{(n-|m|)!}{n!}}L_{n-|m|}^{|m|}(4p_0^2).$$

For now, we focus only on transitions that are almost energy conserving. This step is justified below. Given this assumption, the coupling between atom and resonator depends only on the matrix element $\langle n|A|n+1\rangle$, i.e., $m = 1$. Choosing $\theta = \pi/2$ reproduces the well-known $\sqrt{n}$ behavior of the Jaynes-Cummings model. However, for $\theta < \pi/2$ the matrix element shows a nonmonotonous dependence of the number n of photons in the resonator (inset in Fig. 1). In particular, there are photon numbers n_0 where the matrix element is close to zero. There, the atom is not able to further increase the number of photons in the resonator. As discussed in the next section, this is accompanied by a squeezed photon distribution.

III. PHOTON STATISTICS

We calculate the photon statistics of the laser analogously to Ref. [36]: The system is described by the master equation for its density matrix ρ,

$$\dot\rho = -\frac{i}{\hbar}[H_\mathrm{p},\rho] + L_\mathrm{R}\rho + L_\mathrm{Q}\rho. \qquad (4)$$

The Lindblad superoperators are given by

$$L_\mathrm{R}\rho = \frac{\kappa}{2}(2a\rho a^\dagger - a^\dagger a\rho - \rho a^\dagger a), \qquad (5)$$
$$L_\mathrm{Q}\rho = \frac{\Gamma_\downarrow}{2}(2\sigma_-\rho\sigma_+ - \rho\sigma_+\sigma_- - \sigma_+\sigma_-\rho)$$
$$+ \frac{\Gamma_\uparrow}{2}(2\sigma_+\rho\sigma_- - \rho\sigma_-\sigma_+ - \sigma_-\sigma_+\rho)$$
$$+ \frac{\Gamma_\varphi^*}{2}(\sigma_z\rho\sigma_z - \rho), \qquad (6)$$

where κ is the damping rate of the resonator, $\Gamma_\uparrow$ and $\Gamma_\downarrow$ are the effective pumping rates between the lasing states (including relaxation effects), and Γ_φ^* is the pure dephasing rate of the atom. We show below that this form of the Lindblad superoperators is a good approximation even after the polaron transformation.

We derive an effective equation of motion for the reduced density matrix of the resonator,

$$\rho_\mathrm{r} = \mathrm{Tr}_\mathrm{atom}(\rho),$$

where the trace is only taken over the atomic states. Tracing out the atomic states in Eq. (4) yields

$$\dot{\rho}_{\mathrm{r}} = -\frac{i}{\hbar}[\hbar\omega a^{\dagger}a,\rho_{\mathrm{r}}] - \frac{i}{\hbar}\mathrm{Tr}_{\mathrm{atom}}[(\sigma_+ A + \sigma_- A^{\dagger}),\rho] + L_{\mathrm{R}}\rho_{\mathrm{r}}. \tag{7}$$

To evaluate the second term, we need to solve the remaining equation of motion for ρ,

$$\dot{\rho} = -\frac{i}{\hbar}[H_{\mathrm{p}},\rho] + L_{\mathrm{Q}}\rho.$$

We write this as a system of four coupled differential equations for the matrix elements of all possible combinations of atomic states. The matrix elements are denoted by $\rho_{r\,p,s\,q} = \langle p|\langle r|\rho|s\rangle|q\rangle$ with $r,s \in \{\uparrow,\downarrow\}$ and $p,q \in \mathbb{N}_0$. If $\rho_{\downarrow p,\downarrow q}$ and $\rho_{\uparrow p+1,\uparrow q+1}$ are eliminated using $(\rho_{\mathrm{r}})_{p,q} = \rho_{\uparrow p,\uparrow q} + \rho_{\downarrow p,\downarrow q}$, the system can be cast into the form

$$\dot{\vec{R}} = M\cdot\vec{R} + \vec{A}(\rho_{\mathrm{r}})$$

with

$$\vec{R} = \begin{pmatrix} \rho_{\uparrow p,\uparrow q} \\ \rho_{\uparrow p,\downarrow q+1} \\ \rho_{\downarrow p+1,\uparrow q} \\ \rho_{\downarrow p+1,\downarrow q+1} \end{pmatrix}.$$

M and $\vec{A}(\rho_{\mathrm{r}})$ are given in the Appendix.

The reduced density matrix ρ_{r} of the resonator evolves much more slowly than the density matrix ρ of the whole system. Therefore, we can use an adiabatic approximation and take the stationary solution

$$\vec{R} = -M^{-1}\cdot\vec{A}.$$

Now, the trace in Eq. (7) can be evaluated and ρ_{r} can be calculated. Its diagonal entries

$$\rho(n) = \langle n|\rho_{\mathrm{r}}|n\rangle$$

are the probability distribution of the photon number states in the polaron frame and obey the recursion relation

$$\rho(n) = f(n)\rho(n-1),$$
$$f(n) = \frac{\xi(n-1)\Gamma_{\uparrow}}{\kappa n + \xi(n-1)\Gamma_{\downarrow}}. \tag{8}$$

The parameters are defined as follows:

$$\begin{aligned}
\xi(n-1) &= \frac{\mathcal{A}}{1+\mathcal{B}N(n-1)}\frac{|\langle n-1|A|n\rangle|^2}{\hbar^2 g^2},\\
N(n) &= \frac{\Delta^2}{4g^2}\frac{\Gamma_1}{\frac{\Gamma_1}{2}+\Gamma_{\varphi}^*} + \frac{|\langle n|A|n+1\rangle|^2}{\hbar^2 g^2},\\
\mathcal{A} &= \frac{2g^2}{\Gamma_1\left(\frac{\Gamma_1}{2}+\Gamma_{\varphi}^*\right)},\quad \mathcal{B} = \frac{4g^2}{\Gamma_1\left(\frac{\Gamma_1}{2}+\Gamma_{\varphi}^*\right)},\\
\Delta &= \frac{\epsilon}{\hbar}-\omega,\quad \Gamma_1 = \Gamma_{\uparrow}+\Gamma_{\downarrow}.
\end{aligned} \tag{9}$$

The photon distribution $\rho(n)$ has a local maximum at photon numbers n_{m} with $f(n_{\mathrm{m}}) = 1$ and $f'(n_{\mathrm{m}}) < 0$. Figure 2 compares $f(n)$ for pure σ_x coupling ($\theta = \pi/2$, dashed lines) and generalized couplings (solid lines).

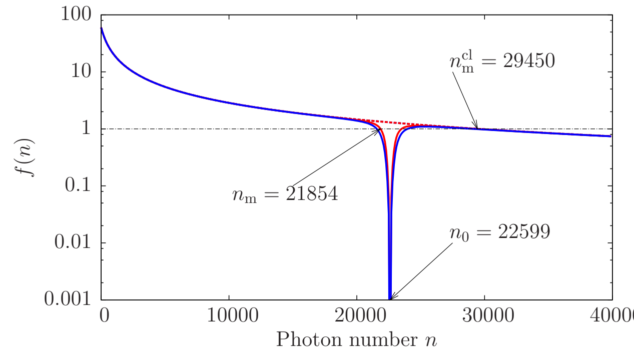

FIG. 2. Recursion coefficient $f(n)$ of the photon statistics $\rho(n) = f(n)\rho(n-1)$ for one atom (red) and 100 atoms (blue). The maximum of $\rho(n)$ is situated at n_{m} defined by $f(n_{\mathrm{m}}) = 1$ and $f'(n_{\mathrm{m}}) < 0$. A conventional laser (pure σ_x coupling, dashed lines) gives $n_{\mathrm{m}}^{\mathrm{cl}} = 29\,450$. In case of both σ_x and σ_z coupling (solid lines), the root of $\langle n|A|n+1\rangle$ at $n_0 = 22\,599$ gives a maximum at much smaller $n_{\mathrm{m}} = 21\,854$ and $n_{\mathrm{m}} = 21\,565$, respectively. As the slope of the solid lines at n_{m} is sharp, a squeezed state is created with $F \ll 1$. Plot parameters are identical to Fig. 1.

For $\theta = \pi/2$, the recursion relation (8) can be solved analytically. Far above the lasing threshold, it is a Poissonian distribution [36]. As $f(n)$ decreases monotonically for $\theta = \pi/2$, there is only one maximum of $\rho(n)$.

For $\theta \neq \pi/2$, $f(n)$ has a root if $\langle n|A|n+1\rangle = 0$. In general, there are now several n_{m} fulfilling the criteria for a local maximum, situated at much smaller photon numbers than the average photon number for $\theta = \pi/2$. The absolute value of the slope $|f'(n_{\mathrm{m}})|$ at these photon numbers is larger than in the case of $\theta = \pi/2$. As discussed in the next section, this yields a photon-number squeezed state.

In principle, there could be several local maxima of $\rho(n)$, but in general only one of these maxima has a probability of the order of unity, unless the lasing parameters are carefully tuned.

IV. FANO FACTOR

We measure the squeezedness of the radiation using the Fano factor F defined by

$$F = \frac{\langle n^2\rangle_{\mathrm{c}} - \langle n\rangle_{\mathrm{c}}^2}{\langle n\rangle_{\mathrm{c}}} \geqslant 0,$$

with $n = a^{\dagger}a$. As introduced above, $|n\rangle_{\mathrm{c}}$ denotes the state with n photons in the resonator cavity. The Fano factor is $F = 1$ if $\rho(n)$ is Poissonian, $F = \langle n\rangle + 1$ if $\rho(n)$ describes a thermal state, and $F < 1$ if $\rho(n)$ describes a photon-number squeezed state.

Expressed by states in the polaron frame, the Fano factor F is

$$F = \frac{\langle n^2 + 2p_0^2 n\rangle - \langle n\rangle^2 + p_0^2}{\langle n\rangle + p_0^2} + \frac{p_0^2\sum_{n=0}^{\infty}(\sqrt{n}\sqrt{n-1}\rho_{n,n-2} + \sqrt{n+1}\sqrt{n+2}\rho_{n,n+2})}{\langle n\rangle + p_0^2}.$$

As $\rho_{n,n\pm 2} \approx 0$ (there are no correlations of different photon-number states) and $p_0^2 = O((\frac{g}{\omega})^2) \ll \langle n\rangle$, we get

$$F \approx F_0 + 2p_0^2,$$

where $F_0 = \frac{\langle n\rangle^2 - \langle n\rangle^2}{\langle n\rangle}$ is now defined in the polaron frame. Given an arbitrary $\rho(n)$, F_0 can be calculated numerically. We show that the value of F_0 depends on the (negative-valued) slope of $f(n)$ at $f(n_\mathrm{m}) = 1$. For that purpose, we linearize $f(n)$ around the maximum photon number n_m, defined by $f(n_\mathrm{m}) = 1$ and $f'(n_\mathrm{m}) = -c$, $c > 0$,

$$f(n) \approx 1 - c(n - n_\mathrm{m}).$$

This approximation is exact near n_m. As $\rho(n)$ drops fast around n_m, deviations from the linearized formula are only large in a region where $\rho(n) \ll 1$. These regions do not contribute to the calculation of the Fano factor. Of course, the approximation can only be used for $n < n_\mathrm{m} + \frac{1}{c}$, as $f(n)$ becomes negative for larger n. A calculation of F_0 using the linearized $f(n)$ yields

$$F_0 = \frac{1}{c}\frac{1}{\langle n\rangle} = \frac{1}{c}\frac{1}{n_\mathrm{m} - 1},$$

which is valid as long as $c \gg e^{-n_\mathrm{m}}$. The steeper $f(n)$ at n_m, the smaller the Fano factor. By tuning the lasing parameters in such a way that $f(n) = 1$ is fulfilled in one of the regions near a root of $\langle n|A|n+1\rangle$ and that $f(n)$ exhibits a sharp slope there, one achieves values $F \ll 1$.

V. MULTIATOM LASING

The number of photons in the resonator can be increased by taking M artificial atoms (with $M > 1$). Therefore, we generalize our model to M identical atoms coupled to a common resonator,

$$H = \sum_{i=1}^{M} \frac{1}{2}\epsilon\sigma_z^i + \hbar\omega a^\dagger a + \hbar g \sum_{i=1}^{M} \big(\cos(\theta)\sigma_z^i + \sin(\theta)\sigma_x^i\big)(a + a^\dagger).$$

The superscript i of the Pauli matrices denotes the atom they act on. The polaron transformation is generalized as well,

$$U = \exp\left[ip\sum_{j=1}^{M}\sigma_z^j\right], \tag{10}$$

and p is defined as above. Transforming H yields

$$\begin{aligned} H_\mathrm{p} = U^\dagger H U &= \sum_{i=1}^{M}\frac{1}{2}\epsilon\sigma_z^i + \hbar\omega a^\dagger a + \sum_{i=1}^{M}(\sigma_+^i A + \sigma_-^i A^\dagger) \\ &\quad - 2x_0 p_0 \sum_{i\neq j=1}^{M}\big(\sigma_+^i\sigma_z^j e^{-2ip} + \sigma_-^i\sigma_z^j e^{2ip}\big) \\ &\quad - \hbar\omega p_0^2 M - \hbar\omega p_0^2 \sum_{i\neq j=1}^{M}\sigma_z^i\sigma_z^j, \end{aligned}$$

where A and $A^\dagger$ are defined as above. The last term introduces correlations between all atoms, and the $\sigma_\pm^i\sigma_z^j$ terms introduce photon-number-dependent couplings between atoms via the $e^{\pm 2ip}$ terms. To solve this, we perform a mean-field approximation,

$$\begin{aligned} \sigma_z^l\sigma_z^j &\approx \sigma_z^l\langle\sigma_z^j\rangle + \langle\sigma_z^l\rangle\sigma_z^j - \langle\sigma_z^l\rangle\langle\sigma_z^j\rangle, \\ \sigma_\pm^i\sigma_z^j &\approx \sigma_\pm^i\langle\sigma_z^j\rangle + \langle\sigma_\pm^i\rangle\sigma_z^j - \langle\sigma_\pm^i\rangle\langle\sigma_z^j\rangle = \sigma_\pm^i\langle\sigma_z^j\rangle, \end{aligned}$$

where in the last step we assumed that only energy-conserving matrix elements of ρ are finite, implying $\langle\sigma_\pm^i\rangle = 0$. Defining

$$S_z^j = \sum_{\substack{i\neq j\\ i=1}}^{M}\langle\sigma_z^i\rangle$$

and assuming that all atoms are identical, we can map the M-atom Hamiltonian on a Hamiltonian analogous to the single-atom case (2) with modified level-splitting energy $\epsilon \to E(S_z^k) = \epsilon - 4\hbar\omega p_0^2 S_z^k$, modified field operators $A \to A(S_z^k) = e^{-ip}xe^{-ip} - 2x_0p_0S_z^k e^{-2ip}$, and an irrelevant constant term. k is the index of an arbitrarily chosen atom. Note that both terms in $A(S_z^k)$ are proportional to e^{-2ip}, so that the roots of the coupling matrix elements are not changed, but the steepness of the recursion coefficient $f(p)$ changes (Fig. 2).

Calculating the photon statistics, there is a change in $\xi(n-1)$ due to the increased number of atoms and the modified field operators,

$$\begin{aligned} \xi(n-1) &= M\frac{\mathcal{A}}{1 + \mathcal{B}N(n-1)}\frac{\left|\langle n-1|A\big(S_z^k\big)|n\rangle\right|^2}{(\hbar g)^2}, \\ \Delta(S_z^k) &= \Delta - 4\omega p_0^2 S_z^k. \end{aligned}$$

Here $\mathcal{A}$, $\mathcal{B}$ are unchanged, and in $N(n)$ the replacements $A \to A(S_z^k)$ and $\Delta \to \Delta(S_z^k)$ have to be made.

Once ρ is known, S_z^k can be determined self-consistently from

$$S_z^k = (M-1)D_0 - \frac{M-1}{M}\frac{2\kappa}{\Gamma_1}\langle n\rangle,$$

with $D_0 = \frac{\Gamma_\uparrow - \Gamma_\downarrow}{\Gamma_\uparrow + \Gamma_\downarrow}$ being the stationary atom polarization.

VI. HIGHER-ORDER RATES

In the previous discussion, we focused only on energy-conserving transitions in the Hamiltonian. However, the matrix elements $\langle n|A|n+m\rangle$ are in fact nonzero for $m \neq 1$. But we show that there is a range of lasing parameters where energy-nonconserving processes are suppressed.

Energy-nonconserving transitions might drive the system across the squeezing point n_0 where $\langle n_0|A|n_0+1\rangle = 0$. Therefore, we want the corresponding transition rates to be small at n_0. Near n_0, we can solve the master equation containing the energy-nonconserving two-photon rates $\langle n|A|n+2\rangle$ while the one-photon rates $\langle n|A|n+1\rangle$ vanish. The rate for a two-photon transition near n_0 is

$$\begin{aligned} \Gamma_{p\to p+2} &= \frac{M\mathcal{A}}{1 + \mathcal{B}\bar{N}(p)}\frac{\left|\langle p|A\big(S_z^k\big)|p+2\rangle\right|^2}{(\hbar g)^2}\Gamma_\uparrow, \\ \bar{N}(p) &= \frac{\big(\Delta(S_z^k) - \omega\big)^2}{4g^2}\frac{\Gamma_1}{\frac{\Gamma_1}{2} + \Gamma_\varphi^*} + \frac{\left|\langle p|A\big(S_z^k\big)|p+2\rangle\right|^2}{(\hbar g)^2}. \end{aligned}$$

If the master equation is solved taking into account only the energy-conserving transitions, the corresponding formula for the one-photon rate is

$$\Gamma_{p\to p+1} = \frac{M\mathcal{A}}{1+\mathcal{B}N(p)}\frac{|\langle p|A|p+1\rangle|^2}{\hbar^2 g^2}\Gamma_\uparrow,$$

where $N(p)$ is defined in Eq. (9). We now try to modify the lasing parameters g and θ in order to suppress the two-photon rate. As we want n_0 to be fixed, p_0 has to be constant. This reduces the parameter space (g,θ) to a one-dimensional one, implying $g(\theta) = p_0\frac{\omega}{\cos(\theta)}$, and yields the following structure of the transition rates:

$$\Gamma_{p\to p+1} = \frac{p_0^2\,\omega^2\tan^2(\theta)\,X_1(p,1)}{1+\Delta^2 X_2 + p_0^2\,\omega^2\tan^2(\theta)\,X_3(p,1)},$$

$$\Gamma_{p\to p+2} = \frac{p_0^4\,\omega^2\tan^2(\theta)\,X_1(p,2)}{1+(\Delta-\omega)^2 X_2 + p_0^4\,\omega^2\tan^2(\theta)\,X_3(p,2)},$$

with $X_2 = (\frac{\Gamma_1}{2}+\Gamma_\varphi^*)^{-2}$ being a constant and $X_1(n,m)$ and $X_3(n,m)$ being functions containing parts of the matrix elements $\langle n|A|n+m\rangle$. Because of $\omega^2 X_2 \gg 1$, for $\Delta = 0$ the rates are given by

$$\Gamma_{p\to p+1} = \frac{p_0^2\,\omega^2\tan^2(\theta)\,X_1(p,1)}{1+p_0^2\,\omega^2\tan^2(\theta)\,X_3(p,1)},$$

$$\Gamma_{p\to p+2} = \frac{p_0^4\tan^2(\theta)\,X_1(p,2)}{X_2+p_0^4\tan^2(\theta)\,X_3(p,2)}.$$

In the limit $\theta\to\pi/2$, both rates are $X_1(p,1)/X_3(p,1) = X_1(p,2)/X_3(p,2) = M\,\Gamma_\uparrow/2$, so there is no suppression. On the other hand, near n_0, for each ω there is a $\theta\to 0$, such that $p_0^2\,\omega^2\tan(\theta)^2 X_3(p,1)\ll 1$ and $p_0^4\tan^2(\theta)X_3(p,2)\ll X_2$. In this limit, we arrive at

$$\Gamma_{p\to p+1} = p_0^2\,\omega^2\,X_1(p,1)\theta^2,$$

$$\Gamma_{p\to p+2} = p_0^4\frac{X_1(p,2)}{X_2}\theta^2 = R(p)\Gamma_{p\to p+1}.$$

The prefactor $R(p)$ is given by

$$R(p) = p_0^2\left(\frac{\frac{\Gamma_1}{2}+\Gamma_\varphi^*}{\omega}\right)^2\frac{X_1(p,2)}{X_1(p,1)}.$$

We chose $p_0 = g\cos(\theta)/\omega \ll 1$ fixed and

$$\frac{X_1(p,2)}{X_1(p,1)} = \frac{16}{p+2}\left(\frac{L_p^2(4p_0^2)}{L_p^1(4p_0^2)}\right)^2$$

is a function of p that diverges at $p=n_0$ and fulfills $X_1(p,2)/X_1(p,1)\lesssim 1$ around n_{m}, where $\rho(n)$ has finite values. So the only way to suppress $R(p)$ is to choose the pumping and dephasing rates small compared to ω. In conclusion, if a secular approximation applies, higher-order transitions are suppressed.

Weak pumping decreases the output power of the laser and the one-photon pumping rate $\Gamma_{p\to p+1}$, which is, however, necessary for the lasing process. In order to compensate for this drop, the number M of atoms has to be enlarged.

As the suppression relies on the case $\theta \ll \pi/2$, a large σ_z coupling to the resonator is needed. Figure 3 illustrates the suppression of the two-photon rate for $\theta = \pi/10$, comparing two cases whose pumping rates differ by one order of magnitude.

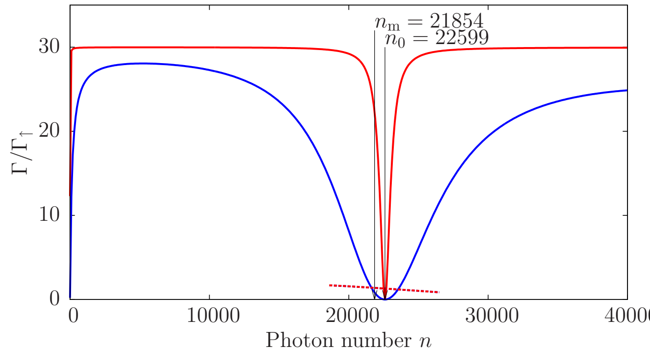

FIG. 3. Comparison of the transition rates from $|\uparrow\rangle$ to $|\downarrow\rangle$ creating one photon (solid lines) or two photons (dashed lines), respectively. For the chosen lasing parameters, the two-photon rates coincide if they are plotted normalized to $\Gamma_\uparrow$. The plot parameters for the red lines are identical to the single-atom case in Fig. 1. The blue lines represent the single-atom case with 10 times larger pumping and dephasing rates, $\Gamma_\uparrow = 0.06$, $\Gamma_\downarrow = 0.001$, and $\Gamma_\varphi^* = 0.01$. The suppression of the two-photon rate for small θ and small pumping rates is visible. Due to our approximations, the plotted two-photon rates are only valid near n_0.

VII. PUMPING PROCESS AND LINDBLAD TERMS

Finally, we show that a pumping process can be implemented and described by a Lindblad term $L_{\mathrm{Q}}\rho$ as given in Eq. (6), containing effective pumping rates $\Gamma_\uparrow$ and $\Gamma_\downarrow$. Furthermore, we show that $L_{\mathrm{R}}\rho$ as given in Eq. (5) is a suitable Lindblad term even after a polaron transformation.

We model the pumping process by two external reservoirs providing the energy for transitions from the lower lasing state $|\downarrow,n\rangle \equiv |\downarrow\rangle|n\rangle$ to an intermediate state $|1,n\rangle$ (at energy ϵ_1) and from there to the upper lasing state $|\uparrow,n\rangle$, respectively. We assume a linear coupling between the reservoirs and the system, $O_{1,\downarrow}X_{1,\downarrow}$ and $O_{1,\uparrow}X_{1,\uparrow}$, where the independent reservoir operators are denoted by $X_{1,\downarrow}$ and $X_{1,\uparrow}$. The Hamiltonian is given by

$$H = H_{\mathrm{S}} + H_{1,\downarrow}^{\mathrm{res}} + H_{1,\uparrow}^{\mathrm{res}} + O_{1,\downarrow}X_{1,\downarrow} + O_{1,\uparrow}X_{1,\uparrow},$$

where H_{S} is given by Eq. (1) supplemented by an additional term $\epsilon_1|1\rangle\langle 1|$ describing the third level required for pumping. The precise form of $H_{1,\uparrow/\downarrow}^{\mathrm{res}}$ and $X_{1,\uparrow/\downarrow}$ does not matter as the bath degrees of freedom will be integrated out. The coupling operators are

$$O_{1,\downarrow} = |1\rangle\langle\downarrow| + |\downarrow\rangle\langle 1|,$$

$$O_{1,\uparrow} = |1\rangle\langle\uparrow| + |\uparrow\rangle\langle 1|.$$

Performing a polaron transformation yields a modified system Hamiltonian $H_{\mathrm{S,p}} = U^\dagger H_{\mathrm{S}} U$ which is given by

$$H_{\mathrm{S,p}} = \tfrac{1}{2}\epsilon\sigma_z + \hbar\omega a^\dagger a + (\sigma_+ A + \sigma_- A^\dagger) + \epsilon_1|1\rangle\langle 1|. \quad (11)$$

The transformed coupling operators are

$$Q_{1,\downarrow} = |1\rangle\langle\downarrow|e^{-ip} + |\downarrow\rangle\langle 1|e^{ip},$$

$$Q_{1,\uparrow} = |1\rangle\langle\uparrow|e^{ip} + |\uparrow\rangle\langle 1|e^{-ip}.$$

Due to the factors $e^{\pm ip}$, matrix elements of $Q_{1,\uparrow/\downarrow}$ creating more than one photon are nonzero. These multiphoton pumping events disturb the creation of squeezed light and must be suppressed.

Integrating out the bath degrees of freedom yields the Bloch-Redfield form of the master equation,

$$\dot{\rho} = -\frac{i}{\hbar}[H_{\mathrm{S,p}},\rho] + \sum_{Q=Q_{1,\downarrow},Q_{1,\uparrow}} (\tilde{Q}_+\rho Q + Q\rho\tilde{Q}_- - Q\tilde{Q}_+\rho - \rho\tilde{Q}_- Q),$$

$$\tilde{Q}_\pm = \int_{-\infty}^{0} d\tau\ \langle X(\pm\tau)X(0)\rangle e^{iH_{\mathrm{S,p}}\tau} Q e^{-iH_{\mathrm{S,p}}\tau},$$

where X is the bath coupling operator associated with Q. For realistic lasing parameters we have $g \ll \omega$. Therefore, a rotating-wave approximation can be performed and the interaction term in $H_{\mathrm{S,p}}$, given by Eq. (11), can be neglected. Then, $|\uparrow/\downarrow,n\rangle$ is an eigenbasis of the remaining Hamiltonian and $\tilde{Q}_\pm$ is given by

$$\langle a,n|\tilde{Q}_\pm|b,m\rangle = \frac{1}{2}S_\pm(\pm(E_{b,m} - E_{a,n}))\langle a,n|Q|b,m\rangle,$$

$$\frac{1}{2}S_+(\Omega) = \int_{-\infty}^{0} d\tau\ \langle X(\tau)X(0)\rangle e^{-i\Omega\tau},$$

$$\frac{1}{2}S_-(\Omega) = \int_{0}^{\infty} d\tau\ \langle X(\tau)X(0)\rangle e^{-i\Omega\tau},$$

$$S(\Omega) = \frac{1}{2}S_+(\Omega) + \frac{1}{2}S_-(\Omega),$$

where $S(\Omega)$ is the spectral function of the bath associated with the coupling operator X, $a,b \in \{\uparrow,\downarrow\}$, and $n,m \in \mathbb{N}_0$.

Higher-order transitions can be suppressed by choosing an appropriate spectral function of the baths. Figure 4(a) shows a sketch of the level diagram in the lasing basis. Choosing $\epsilon_1 > 0$, the system relaxes from $|1,n\rangle$ to $|\uparrow,n\rangle$ releasing an energy $\epsilon_1 - \frac{\hbar\omega}{2}$ into the bath $H_{1,\uparrow}$. A lasing transition is made to $|\downarrow,n+1\rangle$ and from there the system is pumped into the state $|1,n+1\rangle$ taking an energy $\epsilon_1 + \frac{\hbar\omega}{2}$ out of the bath $H_{1,\downarrow}$. Higher-order transitions additionally create or annihilate photons. Therefore, their transition energies differ from $\epsilon_1 \pm \frac{\hbar\omega}{2}$ by an integer multiple of $\hbar\omega$. In order to suppress them, $S_{1,\uparrow}$ and $S_{1,\downarrow}$ must be peaked at $\epsilon_1 \mp \frac{\hbar\omega}{2}$ sharply enough to give small values at all energies differing by an integer multiple of $\hbar\omega$. Obviously, we also have to suppress the decay of the two-level system via the pumping state, which corresponds to the dashed transitions in Fig. 4(a).

Figure 4(b) shows that these conditions can be fulfilled assuming that the pumping is created by a bath with the spectral function of a harmonic oscillator at infinite temperature and the relaxation is a dissipation process with a Lorentzian spectral function,

$$S_{1,\downarrow}(\Omega) = \frac{S_0}{\sqrt{(\Omega^2 - \omega_r^2)^2 + 4\gamma^2\epsilon^2}},$$

$$S_{1,\uparrow}(\Omega) = \frac{S_0'}{\pi}\frac{\gamma'}{(\Omega - \omega_r)^2 + \gamma'^2}.$$

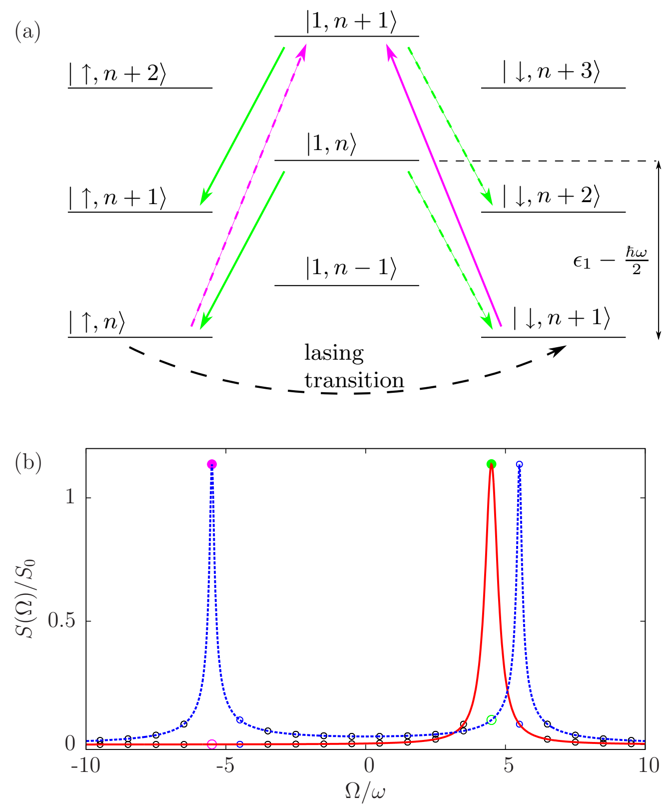

FIG. 4. (a) Level diagram in the lasing basis. Green arrows indicate a release of energy into the bath, and magenta arrows indicate an absorption out of the bath. Dashed transitions have to be suppressed by the spectral function of the baths. (b) Spectral functions $S_{1,\uparrow}$ (solid red) and $S_{1,\downarrow}$ (dashed blue) of the baths. $\epsilon > 0$ means release of energy into the bath, and $\epsilon < 0$ means absorption out of the bath. Solid and open circles indicate desired or suppressed transitions, respectively. The transitions of the pumping process are marked in green and magenta. Black transitions correspond to higher-order processes. Blue circles indicate the transitions of the inverse pumping process. The parameters of the plot are $\epsilon_1 = 5\,\omega$, $\gamma' = 0.28\,\omega$, and $\gamma = 0.08\,\omega$.

Here ω_r denotes the resonance frequencies, which differ for $S_{1,\uparrow}$ and $S_{1,\downarrow}$ by $\hbar\omega$; γ is the damping parameter of the oscillator, γ' the width parameter of the Lorentzian function, and S_0 and S_0' are constants. The pumping can be experimentally realized by using a conventional laser. A suitable setup for the relaxation process was presented recently [37].

Based on these spectral functions, the Bloch-Redfield form of the master equation can be evaluated. We separate terms into those who connect diagonal elements of ρ to either diagonal elements or resonant off-diagonal elements of ρ and all other terms,

$$\dot{\rho} = -\frac{i}{\hbar}[H_{\mathrm{S,p}},\rho] + \sum_n |\langle n|e^p|n\rangle|^2 \Big[S_{1,\downarrow}(-\delta\epsilon_+)|1,n\rangle\langle\downarrow,n|\rho|\downarrow,n\rangle\langle 1,n| + S_{1,\downarrow}(\delta\epsilon_+)|\downarrow,n\rangle\langle 1,n|\rho|1,n\rangle\langle\downarrow,n| - \frac{S_{1,\downarrow}(-\delta\epsilon_+)}{2}(\rho|\downarrow,n\rangle\langle\downarrow,n| + |\downarrow,n\rangle\langle\downarrow,n|\rho)$$

$$
\begin{aligned}
&- \frac{S_{1,\downarrow}(\delta\epsilon_+)}{2}(\rho|1,n\rangle\langle 1,n| + |1,n\rangle\langle 1,n|\rho)\Big]\\
&+ \text{analogous terms for } S_{1,\uparrow}(\pm\delta\epsilon_-)\\
&+ \text{terms connecting off-diagonal matrix elements of } \rho,
\end{aligned} \tag{12}
$$

where $\delta\epsilon_\pm = \epsilon_1 \pm \frac{\hbar\omega}{2}$. All rates have the form $S(\pm\delta\epsilon_\pm)\langle n|e^p|n\rangle\langle m|e^p|m'\rangle$. We show in the next paragraph that all rates to off-diagonal matrix elements of ρ can be neglected using a secular approximation.

Now, a master equation for the two-level system of the lasing transition can be derived. Assuming that the population of the pumping state is constant, $\dot\rho_{1,n;1,n} = 0$, effective transition rates between the lasing states are given by

$$
\begin{aligned}
\Gamma_\uparrow = \Gamma_{|\downarrow,n\rangle\to|\uparrow,n\rangle} &= \frac{\Gamma_{|\downarrow,n\rangle\to|1,n\rangle}\Gamma_{|1,n\rangle\to|\uparrow,n\rangle}}{\Gamma_{|\downarrow,n\rangle\to|1,n\rangle} + \Gamma_{|1,n\rangle\to|\uparrow,n\rangle}}\\
&= \frac{S_{1,\downarrow}(-\delta\epsilon_+)S_{1,\uparrow}(\delta\epsilon_-)}{S_{1,\downarrow}(-\delta\epsilon_+) + S_{1,\uparrow}(\delta\epsilon_-)}|\langle n|e^p|n\rangle|^2,\\
\Gamma_\downarrow = \Gamma_{|\uparrow,n\rangle\to|\downarrow,n\rangle} &= \frac{\Gamma_{|\uparrow,n\rangle\to|1,n\rangle}\Gamma_{|1,n\rangle\to|\downarrow,n\rangle}}{\Gamma_{|\uparrow,n\rangle\to|1,n\rangle} + \Gamma_{|1,n\rangle\to|\downarrow,n\rangle}} \approx 0.
\end{aligned}
$$

$\Gamma_\downarrow$ vanishes as the transition rate $\Gamma_{|\uparrow,n\rangle\to|1,n\rangle}$ is suppressed by the spectral function $S_{1,\uparrow}$. $\Gamma_\uparrow$ and all transition rates in the master equation have a similar structure $O(S(\pm\delta\epsilon_\pm))\langle n|e^p|n\rangle\langle m|e^p|m'\rangle$ and therefore are of the same order of magnitude. Higher-order lasing transitions are suppressed if $\Gamma_\uparrow$, $\Gamma_\downarrow$, $\Gamma_\varphi^* \ll \omega$. This implies that all rates in the master equation (12) are much smaller than ω and, therefore, a secular approximation neglecting all rates to nonresonant off-diagonal matrix elements of ρ holds. The remaining terms of Eq. (12) yield the usual form of the Lindblad superoperator given by the first two lines of Eq. (6) and an irrelevant shift of all atomic energy levels.

Pure dephasing of the atom is treated analogously, using a coupling operator $O_{\rm pd} = \sigma_z$ and one bath. $O_{\rm pd}$ is invariant under a polaron transformation, so the form of the standard Lindblad term for pure dephasing will not change.

The resonator decay is derived with $O_{\rm res} = a + a^\dagger$. Under a polaron transformation, this becomes $Q_{\rm res} = a + a^\dagger - 2p_0\sigma_z$. Again, a secular approximation is performed. The leading two terms yield the Lindblad term of a resonator, whereas the last one gives an additional contribution on pure dephasing with a rate $4p_0^2 S_{\rm res}(0)$.

In conclusion, the form of the Lindblad superoperators assumed in Eqs. (5) and (6) holds even after a polaron transformation, but $\Gamma_\downarrow$, $\Gamma_\uparrow$, and Γ_φ^* are modified effective rates.

VIII. INFLUENCE OF THE MIXING ANGLE ON SQUEEZING

The creation of photon-number squeezing relies on the presence of the σ_z coupling. However, only a certain range of values of the mixing angle θ allows for $F \ll 1$.

The polaron transformation is a nontrivial unitary transformation if $0 \leqslant \theta < \pi/2$. Therefore, the coupling matrix element $\langle n|A|n+1\rangle$ exhibits roots for any of these θ. In order to get photon-number squeezed light, the position of one of these roots, n_0, must be smaller than the maximum photon number $n_{\rm m}^{\rm cl}$ of a conventional laser without σ_z coupling and an effective transversal coupling strength of $g\sin(\theta)$. $n_{\rm m}^{\rm cl}$ is defined by the balance of pumping and loss rates in the system (cf. Fig. 2).

For $\theta \approx \pi/2, n_0 \gg n_{\rm m}^{\rm cl}$ and squeezing is not possible for any set of realistic lasing parameters. For $\theta \gtrsim \pi/4$, $n_0 < n_{\rm m}^{\rm cl}$ might be reached by a suitable parameter choice, but higher-order rates are not suppressed and will drive the system across n_0. Hence the stationary state of the laser will be situated at $n_{\rm m}^{\rm cl}$ and squeezing is not observed. For $\theta \ll \pi/4$, higher-order rates can be suppressed and a photon-number squeezed state can be realized at $\langle n\rangle \approx n_0$. In the extreme case of $\theta \to 0$, the coupling matrix elements vanish as they are proportional to $\sin(\theta)$. This implies that $n_{\rm m}^{\rm cl}$ decreases. On the other hand, $p_0 \to \frac{g}{\omega}$ for $\theta \to 0$. Therefore, n_0 is bounded from below by the position of the root for $p_0 = g/\omega$. Hence, $n_0 > n_{\rm m}^{\rm cl}$ for $\theta \to 0$ and the laser will produce classical radiation at low intensity.

In conclusion, squeezed light is created for $0 < \theta \ll \pi/4$ and there is a tradeoff between good suppression of higher-order rates and sufficient coupling between atom and resonator.

IX. FANO FACTOR IN THE MULTIATOM CASE

In the multiatom case, the polaron transformation is generalized to the one defined in Eq. (10). Therefore, the corrections to the Fano factor due to the polaron transformation change. They give a constraint on the maximum number of atoms if a certain Fano factor should be reached. The correction to the photon number operator due to the polaron transformation is

$$
a_{\rm p}^\dagger a_{\rm p} = a^\dagger a - \xi(a + a^\dagger) + \xi^2, \quad \xi = \sum_{i=1}^{M} p_0\sigma_z^i.
$$

Therefore, the nominator of F is given by

$$
\begin{aligned}
&\langle n^2\rangle_{\rm c} - \langle n\rangle_{\rm c}^2\\
&\quad= \langle n^2\rangle - \langle n\rangle^2 - \langle \xi(a^\dagger a(a + a^\dagger) + (a + a^\dagger)a^\dagger a)\rangle\\
&\qquad + 2\langle a^\dagger a\rangle\langle\xi(a + a^\dagger)\rangle + \langle\xi^2(a^2 + (a^\dagger)^2 + 4a^\dagger a + 1)\rangle\\
&\qquad - \langle\xi(a + a^\dagger)\rangle^2 - 2\langle a^\dagger a\rangle\langle\xi^2\rangle - 2\langle\xi^3(a + a^\dagger)\rangle\\
&\qquad + 2\langle\xi\rangle^2\langle\xi(a + a^\dagger)\rangle + \langle\xi^4\rangle - \langle\xi^2\rangle^2,
\end{aligned}
$$

where the subscript c denotes the cavity frame, as introduced above. Most of the terms cancel due to the following reasons:

(1) The multiatom calculation is performed in a mean-field approximation; therefore, $\langle\xi^r\rangle = \langle\xi\rangle^r$ and $\langle\xi^r\xi a^{(\dagger)}\rangle = \langle\xi\rangle^r\langle\xi a^{(\dagger)}\rangle$ for $r \in \mathbb{N}$.

(2) $\langle\xi a^{(\dagger)}\rangle = 0$ as these terms are proportional to the energy-nonconserving matrix elements $\rho_{\sigma\, n,\sigma\, n\pm1} = 0$, with $\sigma \in \{\uparrow,\downarrow\}$.

The remaining nonvanishing terms are

$$
\langle n^2\rangle_{\rm c} - \langle n\rangle_{\rm c}^2 = \langle n^2\rangle - \langle n\rangle^2 + 4\langle\xi^2 a^\dagger a\rangle + \langle\xi^2\rangle - 2\langle a^\dagger a\rangle\langle\xi^2\rangle.
$$

The expectation values yield in the limit $\langle n\rangle \gg 1$

$$
\begin{aligned}
\langle\xi^2\rangle &= p_0^2 M + p_0^2\frac{M}{M-1}\big(S_z^k\big)^2,\\
\langle\xi^2 a^\dagger a\rangle &= \langle n\rangle\langle\xi^2\rangle - \langle n\rangle p_0^2\frac{2\kappa}{\Gamma_1}S_z^k F_0,
\end{aligned}
$$

where S_z^k is the self-consistent atomic polarization for an arbitrarily chosen atom k and $F_0 = (\langle n^2\rangle - \langle n\rangle^2)/\langle n\rangle$ is the Fano factor of the photon distribution in the polaron frame. In the limit $\langle n\rangle \gg \langle \xi^2\rangle$, the Fano factor is

$$F \approx F_0\left(1 - p_0^2 \frac{8\kappa}{\Gamma_1} S_z^k\right) + 2\langle \xi^2\rangle.$$

If the laser produces classical light, $S_z^k \approx 0$ because the photon number in the cavity is defined by the balance of pumping and loss rates. On the other hand, if the laser produces squeezed light, the number of photons is defined by the root of the coupling matrix element and $S_z^k \lesssim M$. Therefore, we write $S_z^k = \eta M$ with $\eta \in [0,1]$. For typical lasing parameters p_0 and M of the order of 100 we have $p_0^2 M \ll 1$, but $p_0^2 M^2$ is of the order of unity. Therefore, the corrections to the Fano factor due to the polaron transformation can be written as

$$F \approx F_0 + 2p_0^2\eta^2 M^2.$$

The second term of F can be arbitrarily large for large M. If the Fano factor should be smaller than a certain threshold $F_{\max}$ and if p_0 is fixed, we arrive at the constraint

$$M \leqslant \sqrt{\frac{F_{\max} - F_0}{2p_0^2}}.$$

Decreasing p_0 shifts the roots of the coupling matrix element to higher photon numbers and weakens this constraint.

X. CONCLUSION

In this paper we showed that artificial atoms with both σ_x and σ_z coupling offer a way to construct a laser that produces photon-number squeezed light. The maximum photon number can be modified via the coupling strength g and the mixing angle θ. In contrast to other proposals, usual coupling strengths of the order of $1 \times 10^{-3}\omega$ give rise to large photon numbers of the order of 1×10^4. Once a maximum photon number is chosen, g and θ can be adjusted to suppress energy-nonconserving transitions that would otherwise destroy the squeezed state. Furthermore, a pumping process can be implemented using two external baths.

Coupling multiple artificial atoms to a common resonator has already been demonstrated experimentally by the construction of a quantum metamaterial consisting of 20 superconducting flux qubits [22]. The individual qubits exhibited a mixing angle $\theta \approx 1.18$ and a bare coupling strength $g/\omega \approx 5 \times 10^{-5}$ to the third resonator mode at $\omega_3/(2\pi) = 3 \times 2.594$ GHz. In this setup, g/ω is actually quite small. A larger, but still realistic, coupling strength of $g/\omega = 4 \times 10^{-3}$ and a typical resonator decay rate of $\kappa/\omega = 1 \times 10^{-5}$ yield for $M = 200$ atoms and rates of $\Gamma_\uparrow/\omega = 0.05$, $\Gamma_\downarrow/\omega = 0.0001$, and $\Gamma_\varphi^*/\omega = 0.001$ an average photon number of $\langle n\rangle \approx 381\,700$ and a Fano factor $F \approx 0.08$. Hence, using modified qubits with a smaller mixing angle θ, an experimental realization of the presented laser is possible and promising with current qubit technology.

ACKNOWLEDGMENTS

We acknowledge helpful discussions with J. Leppäkangas and G. Schön and funding from the DFG Grant No. MA 6334/3-1.

APPENDIX

The 4×4 matrix M and the vector $\vec{A}$ defined above in the calculation of ρ have the following form ($\hbar = 1$):

$$M = \begin{pmatrix} -i\omega(p-q) - \Gamma_\downarrow - \Gamma_\uparrow & i\langle q+1|A^\dagger|q\rangle & -i\langle p|A|p+1\rangle & 0 \\ i\langle q|A|q+1\rangle & -i\Delta - i\omega(p-q) - \frac{\Gamma_\downarrow}{2} - \frac{\Gamma_\uparrow}{2} - \Gamma_\varphi^* & 0 & -i\langle p|A|p+1\rangle \\ -i\langle p+1|A^\dagger|p\rangle & 0 & i\Delta - i\omega(p-q) - \frac{\Gamma_\downarrow}{2} - \frac{\Gamma_\uparrow}{2} - \Gamma_\varphi^* & i\langle q+1|A^\dagger|q\rangle \\ 0 & -i\langle p+1|A^\dagger|p\rangle & i\langle q|A|q+1\rangle & -i\omega(p-q) - \Gamma_\uparrow - \Gamma_\downarrow \end{pmatrix},$$

$$\vec{A}(\rho_r) = \begin{pmatrix} \Gamma_\uparrow(\rho_r)_{p,q} \\ 0 \\ 0 \\ \Gamma_\downarrow(\rho_r)_{p+1,q+1} \end{pmatrix}.$$

[1] C. M. Caves, Phys. Rev. D **23**, 1693 (1981).

[2] G. S. Agarwal and M. O. Scully, Phys. Rev. A **53**, 467 (1996).

[3] K. Qu and G. S. Agarwal, Opt. Lett. **38**, 2563 (2013).

[4] N. Didier, A. Kamal, W. D. Oliver, A. Blais, and A. A. Clerk, Phys. Rev. Lett. **115**, 093604 (2015).

[5] I. R. Berchera, I. P. Degiovanni, S. Olivares, N. Samantaray, P. Traina, and M. Genovese, Phys. Rev. A **92**, 053821 (2015).

[6] P. A. Knott, W. J. Munro, and J. A. Dunningham, Phys. Rev. A **89**, 053812 (2014).

[7] E. S. Polzik, J. Carri, and H. J. Kimble, Phys. Rev. Lett. **68**, 3020 (1992).

[8] K. Iwasawa, K. Makino, H. Yonezawa, M. Tsang, A. Davidovic, E. Huntington, and A. Furusawa, Phys. Rev. Lett. **111**, 163602 (2013).

[9] J. Miller, L. Barsotti, S. Vitale, P. Fritschel, M. Evans, and D. Sigg, Phys. Rev. D **91**, 062005 (2015).

[10] M. A. Taylor, J. Janousek, V. Daria, J. Knittel, B. Hage, H.-A. Bachor, and W. P. Bowen, Nat. Photon. **7**, 229 (2013).

[11] R. Whittaker, C. Erven, A. Neville, M. Berry, J. L. O'Brien, H. Cable, and J. C. F. Matthews, arXiv:1508.00849.

[12] R. M. Shelby, M. D. Levenson, S. H. Perlmutter, R. G. DeVoe, and D. F. Walls, Phys. Rev. Lett. **57**, 691 (1986).

[13] R. Dong, J. Heersink, J. F. Corney, P. D. Drummond, U. L. Andersen, and G. Leuchs, Opt. Lett. **33**, 116 (2008).
[14] M. Mehmet, H. Vahlbruch, N. Lastzka, K. Danzmann, and R. Schnabel, Phys. Rev. A **81**, 013814 (2010).
[15] R. Vijay, M. H. Devoret, and I. Siddiqi, Rev. Sci. Instrum. **80**, 111101 (2009).
[16] A. Kamal, J. Clarke, and M. H. Devoret, Nat. Phys. **7**, 311 (2011).
[17] F. Mallet, F. R. Ong, A. Palacios-Laloy, F. Nguyen, P. Bertet, D. Vion, and D. Esteve, Nat. Phys. **5**, 791 (2009).
[18] J. Braumüller, J. Cramer, S. Schlör, H. Rotzinger, L. Radtke, A. Lukashenko, P. Yang, S. T. Skacel, S. Probst, M. Marthaler, L. Guo, A. V. Ustinov, and M. Weides, Phys. Rev. B **91**, 054523 (2015).
[19] S. André, L. Guo, V. Peano, M. Marthaler, and G. Schön, Phys. Rev. A **85**, 053825 (2012).
[20] M. Marthaler and M. I. Dykman, Phys. Rev. A **76**, 010102 (2007).
[21] R. Loudon and P. L. Knight, J. Mod. Opt. **34**, 709 (1987).
[22] P. Macha, G. Oelsner, J.-M. Reiner, M. Marthaler, S. André, G. Schön, U. Hübner, H.-G. Meyer, E. Il'ichev, and A. V. Ustinov, Nat. Commun. **5**, 5146 (2014).
[23] L. Childress, A. S. Sørensen, and M. D. Lukin, Phys. Rev. A **69**, 042302 (2004).
[24] W. J. Meath and E. A. Power, Mol. Phys. **51**, 585 (1984).
[25] I. G. Savenko, O. V. Kibis, and I. A. Shelykh, Phys. Rev. A **85**, 053818 (2012).
[26] X. Wang, Q. Liao, H. Li, S. Bai, Y. Wu, X. Lu, H. Hu, Q. Shi, and H. Fu, J. Am. Chem. Soc. **137**, 9289 (2015).
[27] D. A. Rodrigues, J. Imbers, and A. D. Armour, Phys. Rev. Lett. **98**, 067204 (2007).
[28] J. Jin, M. Marthaler, P.-Q. Jin, D. Golubev, and G. Schön, New J. Phys. **15**, 025044 (2013).
[29] M. Marthaler, G. Schön, and A. Shnirman, Phys. Rev. Lett. **101**, 147001 (2008).
[30] M. Marthaler, J. Leppäkangas, and J. H. Cole, Phys. Rev. B **83**, 180505 (2011).
[31] B. Kubala, V. Gramich, and J. Ankerhold, Phys. Scr. **2015**, 014029 (2015).
[32] O. Astafiev, K. Inomata, A. O. Niskanen, T. Yamamoto, Yu. A. Pashkin, Y. Nakamura, and J. S. Tsai, Nature (London) **449**, 588 (2007).
[33] F. Chen, J. Li, A. D. Armour, E. Brahimi, J. Stettenheim, A. J. Sirois, R. W. Simmonds, M. P. Blencowe, and A. J. Rimberg, Phys. Rev. B **90**, 020506 (2014).
[34] G. Oelsner, P. Macha, O. V. Astafiev, E. Il'ichev, M. Grajcar, U. Hübner, B. I. Ivanov, P. Neilinger, and H.-G. Meyer, Phys. Rev. Lett. **110**, 053602 (2013).
[35] Y.-Y. Liu, J. Stehlik, C. Eichler, M. J. Gullans, J. M. Taylor, and J. R. Petta, Science **347**, 285 (2015).
[36] M. O. Scully and M. S. Zubairy, *Quantum Optics* (Cambridge University Press, Cambridge, UK, 1999), Chap. 11.
[37] Z. H. Peng, Y. X. Liu, J. T. Peltonen, T. Yamamoto, J. S. Tsai, and O. Astafiev, Phys. Rev. Lett. **115**, 223603 (2015).